International Journal of Pharmaceutics 645 (2023) 123434

Contents lists available at ScienceDirect

International Journal of Pharmaceutics

journal homepage: www.elsevier.com/locate/ijpharm

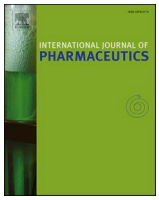

Archaeosomes facilitate storage and oral delivery of cannabidiol

Viktor Sedlmayr [a,1], Christina Horn [b,1], David Johannes Wurm [b], Oliver Spadiut [a], Julian Quehenberger [a,b,*]

[a] TU Wien, Institute of Chemical, Environmental and Bioscience Engineering, Vienna, Austria
[b] NovoArc GmbH, Vienna, Austria

ARTICLE INFO

Keywords:
Archaeosomes
Cannabidiol
Oral drug delivery
Liposomes
Storage stability

ABSTRACT

Cannabidiol (CBD) has received great scientific interest due to its numerous therapeutic applications. Degradation in the gastrointestinal (GI) tract, first-pass metabolism, and low water solubility restrain bioavailability of CBD to only 6% in current oral administration. Lipid-based nanocarriers are delivery systems that may enhance accessibility and solubility of hydrophobic payloads, such as CBD. Conventional lecithin-derived liposomes, however, have limitations regarding stability in the GI tract and long-term storage. Ether lipid-based archaeosomes may have the potential to overcome these problems due to chemical and structural uniqueness. In this study, we compared lecithin-derived liposomes with archaeosomes in their applicability as an oral delivery system of CBD. We evaluated drug load, storage stability, stability in a simulated GI tract, and *in vitro* particle uptake in Caco-2 cells. Loading capacity was 6-fold higher in archaeosomes than conventional liposomes while providing a stable formulation over six months after lyophilization. In a simulated GI tract, CBD recovery in archaeosomes was 57 ± 3% compared to only 34 ± 1% in conventional liposomes and particle uptake in Caco-2 cells was enhanced up to 6-fold. Our results demonstrate that archaeosomes present an interesting solution to tackle current issues of oral CBD formulations due to improved stability and endocytosis.

1. Introduction

Oral delivery is the preferred drug administration route, as it is easy to administer, non-invasive, and is associated with high patient adherence (Alqahtani et al., 2021). However, the physicochemical and pharmacokinetic properties of the drug often restrict the efficiency of oral medication (Lin and Wong, 2017). Drugs have to surpass the gastrointestinal (GI) tract, where exposure to the low pH environment of the stomach, bile salts, and digestive enzymes may lead to degradation. Transportation of the drug to the blood circulation is critical since several drugs exhibit low mucosal permeability and/or are preferentially absorbed via the portal vein to experience extensive first-pass metabolism in the liver (Ahn and Park, 2016). Considering that the most common drug candidates are poorly water-soluble, the dissolution step is challenging (Kok et al., 2022). Low water solubility triggers the precipitation of the drug in the stomach, thereby decreasing bioavailability (Millar et al., 2020).

Cannabidiol (CBD), a major non-psychotropic component of the Cannabis plant, is a highly lipophilic cannabinoid with numerous therapeutic properties. Anti-tumor (Hinz and Ramer, 2019), anti-inflammatory (Atalay et al., 2019), neuroprotective (Silvestro et al., 2019), and analgesic effects (Cristino et al., 2020) are explained by its interaction with the endocannabinoid system (ECS), being a low-affinity binding CB_1 agonist/ CB_2 inverse agonists (Thomas et al., 2007). Furthermore, recent *in vivo* and *in vitro* studies promise the application of CBD as a potent antibiotic against resistant bacterial strains (Abichabki et al., 2022; Blaskovich et al., 2021) and in treating viral infections (Khodadadi et al., 2020). Besides being an active component in a wide range of products in the cosmetic and food industry, the therapeutic potency of CBD caused the approval of two pharmaceuticals. In 2010, the first CBD-containing drug Sativex®, used for the treatment of multiple sclerosis-related spasticity, was approved by the Medicines and Healthcare products Regulatory Agency. Even though Sativex® is classified as an oromucosal spray, a substantial proportion of CBD is transported via the GI tract (Itin et al., 2019). Later in 2018, Epidiolex®, the first drug with CBD as the sole active component used in the treatment of rare forms of epilepsy, was approved by the Food and Drug Administration. Both drugs are cannabinoid oil products incorporating

* Corresponding author at: Institute of Chemical, Environmental and Bioscience Engineering, TU Wien, Vienna, Austria.
E-mail address: julian.quehenberger@tuwien.ac.at (J. Quehenberger).
[1] These authors contributed equally.

https://doi.org/10.1016/j.ijpharm.2023.123434
Received 23 May 2023; Received in revised form 15 August 2023; Accepted 19 September 2023
Available online 20 September 2023

CBD at a high concentration, compensating for the bioavailability of only 6% of current oral CBD oil formulations (Perucca and Bialer, 2020). The low absorption of CBD is ascribed to the precipitation of the drug in the stomach (Millar et al., 2020), degradation and conversion in gastric fluids (Merrick et al., 2016), and a prominent first-pass metabolism (Franco et al., 2020). These effects generate large intra- and inter-subject variability, further intensified by relevant food effects (Birnbaum et al., 2019).

A strategy to enhance the oral bioavailability of hydrophobic substances, like CBD, is the utilization of the lymphatic transportation system rather than the uptake by the portal vein. This route surpasses clearance via the first pass effect in the liver and enables the drug transport into the blood system via the lymph. Lipid-based nanocarriers (LBNs) are delivery systems of poorly water-soluble substances which enhance the absorption of orally administered drugs by increasing solubility in GI fluids and improving such lymphatic drug transport (Franco et al., 2020; Porter et al., 2007). Liposomes are spherically-shaped LBNs composed of phospholipid bilayers that enhance the solubility of hydrophobic drugs and can be designed to target the intestinal lymphatic system (Singh et al., 2020). Plant- and animal-derived phosphatidylcholines in mixtures with cholesterol are commonly used to formulate liposomes to encapsulate poorly water-soluble drugs (Crommelin et al., 2020; Fricker et al., 2010). Enzymatic degradation by GI lipases and hydrolysis, however, limits the stability of conventional liposomes in oral applications. Archaeosomes, incorporating biologic or synthetic ether lipids instead of conventional ester lipids, represent a liposome class characterized by high resistance against phospholipase activity, oxidation, physical conversion (e.g. fusion and aggregation), hydrolysis, and bile salts (Rastädter et al., 2020; Kaur et al., 2016). They expose high membrane rigidity due to the incorporation of bipolar tetraether lipids, forming lipid monolayers and not lipid bilayers (Hemetsberger et al., 2022; Schilrreff et al., 2019). These structural characteristics of archaeosomes have been shown to improve the GI stability of delivery vehicles for proteins, peptides, and water-insoluble compounds (Uhl et al., 2016; Parmentier et al., 2014; Li et al., 2010) and facilitate mucosa permeability of drugs (Parmentier et al., 2011). Parmentier et al. found a substantial share of radiolabeled ether lipids after oral administration of archaeosomes made in mixtures with conventional phospholipids in the GI tract and in excretions of mice. From this, the authors hypothesized an uptake mechanism of drug release via adsorption of archaeosomes to enterocytes before drug leakage into the blood stream (Parmentier et al., 2011). On the other hand, Morilla et al. recovered a significant amount of radiolabeled DTPA, a substance exhibiting very low permeability in the intestine, encapsulated in archaeosomes prepared from lipids from *Halorubrum tebenquichense*, in the blood of rats. The authors ascribed this observation to the uptake of intact archaeosomes by enterocytes, while drug leakage occurs during transcytosis (Morilla et al., 2011). Hence, it is still unclear if the drug absorption occurs via a para- or transcellular transportation, via an adsorption mechanism or via a combination of the three processes. Studies have confirmed the efficiency of oral archaeosomal administration, which can be associated with a prolonged retention time in the GI tract and a prominent uptake by M cells (Romero and Morilla, 2023; Kaur et al., 2016). LBNs consisting of ether lipids could therefore also enhance the bioavailability of CBD by providing stability in the GI tract, facilitating mucosal penetration, and enabling the lymphatic uptake of the drug (Jia et al., 2022; Uhl et al., 2016).

Hence, due to their extraordinary stability, archaeosomes have the potential to solve the current issues associated with the oral administration of CBD. Beyond that, the limited storage stability of commercial CBD products (56 days for Epidiolex®/ 48 days for Sativex® after opening the container) has been described as another major issue (Millar et al., 2020). Distinct storage aspects of archaeosomes could enable a more robust CBD formulation (Kaur et al., 2016).

In this study, we prepared conventional soybean lecithin-derived liposomes (Tiboni et al., 2021) and archaeosomes, incorporating ether lipids from the thermoacidophilic archaeon *Sulfolobus acidocaldarius*, using a state-of-the-art microfluidic formulation technique. The formulations were characterized regarding their physical properties (size, size distribution, encapsulation efficiency, Zeta potential, cryo-TEM analysis). We furthermore investigated the stability of the LBNs in solution and after lyophilization during storage at room temperature and under light exposure over six months, as well as in an accelerated oxidation assay. Moreover, the applicability of archaeosomes and SPC/Chol liposomes as an oral CBD delivery system was assessed in a simulated GI tract and in an *in vitro* particle uptake assay using Caco-2 cells as a model cell line for enterocytes.

2. Materials and methods

2.1. Chemicals and reagents

Archaeal lipid extract was provided by NovoArc GmbH (Austria). It consists of a mixture of diether- and tetraether lipids with various headgroups, mainly inositol phosphate and mono- and dihexoses (Quehenberger et al., 2020). CBD was acquired from PhytoLab (Germany) in solid form with a purity of > 99%, and Phospholipon® 90 G (SPC) was kindly supplied by Lipoid (Germany). Cholesterol and 1,2-dipalmitoyl-*sn*-glycerol-3-phosphoethanolamine-*N*-(lissamine rhodamine B sulfonyl) (ammonium salt) (16:0 Liss Rhod PE) were purchased from Avanti Polar Lipids, Inc (USA). RGE-15 (rabbit gastric extract) was obtained from LipolyTech (France). All solvents (ethanol, 2-propanol, dimethyl sulfoxide), pancreatin, and bile salts were obtained from Sigma Aldrich (USA) or Roth (Germany). Solvents for HPLC analysis were purchased from PanReac AppliChem ITW Reagents (Germany).

2.2. Formulation of liposomes and archaeosomes

Liposomes and archaeosomes were formulated using a Nano-Assemblr Ignite (Precision Nanosystems Inc., Canada). The preparation parameters were chosen as described earlier (Tiboni et al., 2021). LBNs were formulated at a total lipid concentration of 15 g/L in the organic phase. The organic phase for liposomes consisted of SPC:cholesterol (3:1, w/w) dissolved in ethanol, while archaeal lipids for archaeosomes were dissolved in a mixture of dimethyl-sulfoxide: 2-propanol (2:3, v/v). SPC liposomes without cholesterol were prepared at 15 g/L SPC in the organic phase. For rhodamine-labeled LBNs, a total concentration of 13 μM of 16:0 Liss Rhod PE was added to the organic phase. All formulations were prepared at a total flow rate of 12 mL/min and with 10 mM phosphate buffer saline (PBS) at pH = 7.4 as the aqueous phase. The flow rate ratio (FRR) was varied between 3:1 and 2:1 (aqueous phase: organic phase), and CBD concentration in the organic phase was varied between 0.4 and 2 g/L. After formulation, samples were diluted 1:3 with 10 mM PBS (pH = 7.4) before dialysis (dialysis membrane Spectra/Por 1, MWCO 6–8 kDa (Repligen, USA)) was carried out overnight. Formulations were performed in triplicates.

2.3. Physicochemical characterization of CBD archaeosomes and liposomes

Dynamic light scattering and Zeta potential

Particle size and polydispersity index (PDI) were determined by dynamic light scattering with a ZetaSizer Nano ZS (Malvern Panalytical Ltd Instruments, United Kingdom) (cell type: ZEN0040; T: 25 °C; nr. of measurements: 3; nr. of runs: 11; run duration: 10 s; measurement angle: 173° backscatter). Zeta potential measurements were conducted on the same device (Cell type: DTS1070; T: 25 °C; nr. of measurements: 3; nr of runs: 100).

Encapsulation efficiency

The concentration of CBD was determined via reversed phase HPLC analysis on a Vanquish Flex HPLC system (Thermo Fisher Scientific, USA). Separation of analytes was carried out on an Accucore C18 (150 × 3 mm, 2.6 μm; Thermo Fisher Scientific, USA). The mobile phase was

composed of (A) ultrapure water + 0.1% (v/v) trifluoroacetic acid and (B) acetonitrile + 0.1% (v/v) trifluoroacetic acid. The flow rate was set to 0.8 mL/min, and the column temperature was 60 °C. Elution was achieved by a stepwise increase of buffer B: after an equilibration step at 20% (B) for 1.5 min, analytes were eluted at 75% (B) for 3.5 min, followed by a 2 min washing step at 95% (B). The column was re-equilibrated for 3 min at 20% (B). Detection of CBD was carried out at 220 nm, while a 3D field (190–500 nm) was applied to identify oxidation products. Encapsulation efficiency (EE%) was calculated as follows:

EE%= concentration of CBD (after dialysis)/concentration of CBD (before dialysis) *100%

HPLC method validation was conducted to assess reliability, precision, and accuracy for the quantification of CBD. Standard solutions were prepared by serial dilution from a single stock in the range of 3–200 mg/L and measured in triplicates. The injection volume was set to 1 μL. The limit of detection was determined to be 0.7 mg/L, and the limit of quantification was found to be 2.1 mg/L. For the evaluation of precision, four different CBD standards (3, 12.5, 50, and 100 mg/L) were measured on six separate days, resulting in a%Precision of 2% (RSD). Accuracy was measured by spiking a total concentration of 40 mg/L, respectively 20 mg/L to the standards. Average %Accuracy was 102%.

2.4. Cryo-transmission electron-microscopy

Cryo-transmission electron microscopy (TEM) analysis was performed to determine the morphology of CBD archaeosomes. Sample volumes of 4 μL were applied to Cu 200 mesh R2/2 holey carbon grids (Quantifoil, Germany) and loaded into a Leica GP (Leica Microsystems, Austria) grid plunger with the climate chamber set to 20 °C and 75% relative humidity. After blotting for 1-, 2- and 4-seconds, grids were plunge-frozen in liquid ethane at approximately −180 °C for instant vitrification. Cryo-samples were transferred to a Glacios cryo-transmission microscope (Thermo Scientific, USA) equipped with an X-FEG, and images were recorded in low-dose mode using the SerialEM software (Mastronarde, 2005) with a Falcon3 direct electron detector in low-dose mode at a magnification of 150,000 and a pixel size of 0.9858 Å. Evaluation of the thickness of the monolayer was estimated by measuring the length of the membrane of 35 different particles using ImageJ 1.53 t (Schneider et al., 2012).

2.5. Accelerated oxidation study and long-term storage of CBD archaeosomes and liposomes

Stability against oxidative and basic conditions was evaluated by adding 100 mM KOH to a final pH = 10 (Mechoulam and Hanuš, 2002) and incubation of samples in a thermostated autosampler at 40 °C for 48 h. A sample was analyzed via HPLC every hour to monitor the degradation process. The free CBD was generated by dissolving CBD in DMSO and performing a 1:5 dilution in 10 mM PBS (pH = 7.4) to get a final CBD concentration of 0.40 g/L.

Lyophilization was conducted by performing a 1:2 dilution with a 400 mM sucrose solution as a cryo-protectant, shock-freezing the mixtures in liquid nitrogen, and lyophilization for 48 h on a FreeZone 2.5 Liter Benchtop Freeze Dry System (Labconco, USA). Lyophilized samples and samples in solution were stored under exposure to daylight and at room temperature and analyzed after 1, 4, and six months. Before analysis, lyophilized LBNs were rehydrated using ultrapure water in the original sample volume.

2.6. Stability of CBD archaeosomes and liposomes in a simulated digestion system

The INFOGEST 2.0 method (Brodkorb et al., 2019) was performed to investigate the stability of archaeosomes and liposomes in gastric and intestinal fluids. Archaeosomes and liposomes were exposed to a simulated human digestion process over 4 h, including an oral, gastric, and intestinal phase. Oral (SSF, simulated salivary fluid), gastric (SGF, simulated gastric fluid), and intestinal (SIF, simulated intestinal fluid) fluids with varying salt concentrations were prepared. Pepsin and gastric lipase were added to the gastric phase, whereas pancreatin and bile salts were added to the intestinal phase. CBD LBNs were mixed with SSF (1:1; v/v) and incubated at 37 °C at 330 rpm for 2 min, followed by the addition of SGF in a ratio 1:1 (v/v) to the SSF-samples and incubation at 37 °C (330 rpm) for 2 h. Enzymes were inactivated by the addition of 0.1 M NaOH after 2 h. In the intestinal phase, the SSF SGF samples were diluted 1:2 with SIF and incubated at 37 °C for 2 h. The addition of a Bowman-Birk inhibitor and 4-bromophenylboronic acid achieved the inactivation of the enzymes. The decay of CBD during each phase was determined via HPLC analysis.

2.7. In vitro particle uptake in Caco-2 cells

Caco-2 cells were seeded in 48 well plates at a cell density of $8*10^4$ cells/well in 950 μL medium (Minimum Essential Medium (MEM) + L-glutamine, 10% fetal bovine serum (FBS), 1% antibiotic mix). Cell concentration was determined on an EVE™ Automated Cell Counter (NanoEnTek, South Korea). After 24 h of incubation (37 °C, 5% CO_2), 50 μL of LBN sample after completion of the simulated digestion system were added to the wells at a concentration of 1 μM 16:0 Liss Rhod PE. PBS (pH = 7.4) was included as a blank. After incubation for 4, 8, and 24 h, cells were washed twice with 10 mM PBS buffer to remove liposomes remaining in the supernatant. This was followed by adding 300 μL of Hoechst solution (1 μg/mL) and an incubation step of 20 min (37 °C, 5% CO_2). After two washing steps with 10 mM PBS buffer, particle uptake was determined by measuring the fluorescence intensity of rhodamine-labeled archaeosomes and SPC/Chol liposomes(excitation/emission = 570 nm/590 nm) and the number of cell nuclei (excitation/emission = 460 nm/ 490 nm) by confocal microscopy (IX83, Olympus, Japan). Data evaluation was performed with ImageJ 1.53 t (Schneider et al., 2012). The *in vitro* particle uptake assay was performed with three individual formulations for archaeosomes and liposomes after formulations and

Table 1
Physicochemical characterization of soybean lecithin-based liposomes (SPC/Chol liposomes) and archaeosomes. Conventional liposomes (SPC/Chol) consisted of a mixture of Phospholipon® 90 G and cholesterol (3:1, w/w), while a pure archaeal lipid extract was used to prepare archaeosomes. Theoretical CBD concentration was calculated considering the dilution of CBD in the organic phase caused by the flow rate ratio (FRR). A polydispersity index (PDI) < 0.2 indicates monodisperse distribution of the particles (Khadke et al., 2020).

	SPC/Chol liposomes0.4 g/L CBD FRR = 3:1	**Archaeosomes 0.4 g/L CBD FRR = 3:1**	**Archaeosomes 2 g/L CBD FRR = 3:1**	**Archaeosomes 2 g/L CBDFRR = 2:1**
Theoretical CBD concentration (g/L)	0.10	0.10	0.50	0.67
Encapsulation efficiency (%)	90 ± 2	93 ± 3	97 ± 2	95 ± 1
Particle size (nm)	77 ± 2	83 ± 1	84 ± 0.0	88 ± 2
PDI	0.107 ± 0.027	0.141 ± 0.010	0.040 ± 0.005	0.050 ± 0.017
Z-Potential / mV	−3.6 ± 0.6			−25.6 ± 1.4

with LBNs (in solution/lyophilized) after six months of storage, as described above.

2.8. Statistical analysis

Data were analyzed using Python 13.11.4 software employing an unpaired Student's *t*-test. A *P*-value of ≤ 0.05 was considered statistically significant and denoted with a single asterisk (*), while ** indicated a *P*-value ≤ 0.01. The results were represented as mean $\pm$ standard deviation.

3. Results and discussion

3.1. Physicochemical characterization of CBD archaeosomes and liposomes

CBD liposomes were prepared using microfluidic techniques as described earlier (Tiboni et al., 2021). CBD was encapsulated at an initial concentration of 0.40 g/L in an SPC:cholesterol mixture (3:1, w/w) at a flow rate ratio (FRR) of 3:1 (aqueous phase: organic phase) (SPC/Chol liposomes). Archaeosomes were prepared using the same formulation conditions. At 100% encapsulation efficiency, these formulations yield a theoretical CBD concentration of 0.10 g/L. Both formulations delivered monodisperse LBNs with a similar encapsulation efficiency of around 90% (Table 1). In accordance with previous studies, archaeosomes exhibited a slightly larger particle diameter than SPC/Chol liposomes (Li et al., 2010) below a particle diameter of 100 nm, which has been shown to facilitate lymphatic uptake (Jia et al., 2022). Since high drug loading capacity is essential for a feasible formulation (Shen et al., 2017), two parameters were varied to increase CBD content in the final product: 1) enhancement of the initial CBD concentration in the organic phase, and 2) reduction of the dilution during the formulation by reducing FRR. Initial CBD concentration was increased from 0.4 g/L to 2 g/L, while FRR was reduced from 3:1 to 2:1. In the case of SPC/Chol liposomes, the increase of CBD content and share of the organic phase caused a disturbance in the lipid self-assembly, leading to the precipitation of lipids and CBD. Formulation of SPC/Chol liposomes at FRR = 2:1 and 0.4 g/L CBD resulted in the same observation. The encapsulation efficiency of all formulations was high. Independent of the applied FRR, encapsulation efficiency for archaeosomes was increased up to 97% compared to the lower CBD load. Interestingly, the increase of CBD content in the organic phase caused a reduction of the PDI. The differences regarding payload can be ascribed to the incorporation of cholesterol in conventional liposome formulations, which occupy similar regions in the lipid bilayer as CBD. Nevertheless, for conventional liposomal formulations cholesterol is an obligatory constituent since omitting cholesterol leads to structural instability of conventional liposomes and consequently precipitation of the particles (data not shown). For archaeosomes, both strategies could be applied successfully, enabling to increase CBD concentration by a factor of 6.7 to 0.67 g/L. Similar trends considering the influence of a decreased FRR on the particle size, triggering an increase of the particle diameter, were observed in a previous studies (Jia et al., 2022). A possible explanation for the higher payload is the intrinsic rigidity of archaeosomes caused by monolayer-spanning tetraether lipids, ensuring membrane integrity and packaging, eventually enabling a higher drug loading capacity (Nakhaei et al., 2021). Table 1 summarizes the results of the physical characterization of the CBD archaeosomes and CBD SPC/Chol liposomes.

Based on the results presented in Table 1, the following experiments were conducted with SPC/Chol liposomes, prepared at an initial CBD concentration of 0.40 g/L and an FRR of 3:1 and archaeosomes, formulated at 2.00 g/L initial CBD in the organic phase at an FRR of 2:1. Zeta potential of the formulations were -3.6 ± 0.6 mV (SPC/Chol liposomes) and -25.6 ± 1.4 mV (archaeosomes).

TEM analysis of CBD archaeosomes (2 g/L CBD; FRR = 2:1) revealed that the spherical LBNs are composed of a monolayer surface with a solid inner core (Fig. 1). The mean thickness of the monolayer, derived from the graphical evaluation of the TEM images, was 4.9 ± 0.7 nm, consistent with the thickness of stretched tetraether lipid membranes (Chong et al., 2022). Similar morphologies, as seen in Fig. 1, were observed for diether lipid-based formulations using microfluidic techniques in mixtures with hollow core compartment forms (Jia et al., 2022). In that study, the authors ascribed the presence of solid compartments to the formation of solid lipid nanoparticles (SLNs) associated with anti-solvent precipitation during the mixing. The inner core may contribute to the higher drug-loading capacity of archaeosomes observed in this study.

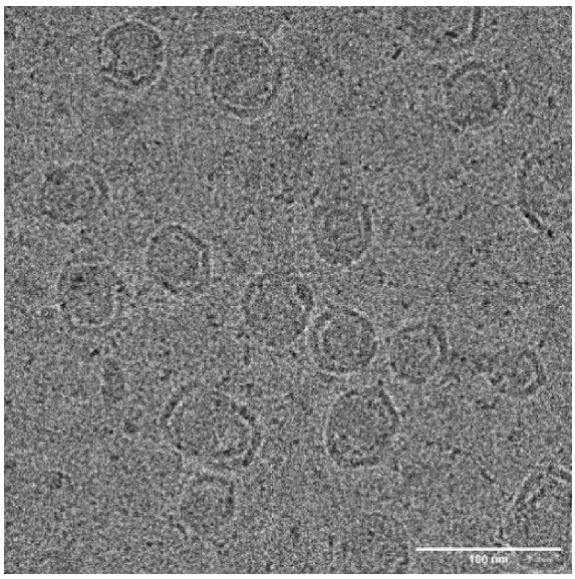

Fig. 1. TEM images of cannabidiol (CBD) archaeosomes in 150,000 × magnification. A clear separation between the lipid bilayer and the solid inner core structure can be observed. The scale bar corresponds to 100 nm.

3.2. Accelerated oxidation study and long-term storage of CBD liposomes and archaeosomes

CBD shows low stability during storage, and degradation is accelerated by light exposure, auto-oxidation, and temperature. Decay of aqueous and oil-based CBD preparations is observable after 14 days of storage, with CBD degradation of up to 75% in aqueous solutions (Pacifici et al., 2017). The decomposition of CBD is of high relevance, as acidic (caused by carbon dioxide from the air) and basic conditions lead to a transformation to psychotropic cannabinoids, like Δ^9-tetrahydrocannabinol (Δ^9-THC) and Δ^8-THC respectively Δ^6-CBD (Citti et al., 2021; Golombek et al., 2020). To assess the degradation of SPC/Chol liposomes and CBD archaeosomes, we first performed an accelerated oxidation study at an elevated temperature of 40 °C and high pH. Unencapsulated CBD served as a reference. Fig. 2A shows the decay of CBD over 40 h. CBD content in the SPC/Chol samples dropped to 50 ± 2%, indicating a similar course of CBD decay as the unencapsulated sample (48 ± 1% after 40 h). In archaeosomes, 64 ± 3% of CBD was recovered. Hence, under basic conditions, CBD degradation in archaeosomes is reduced substantially. We further investigated the long-term storage stability of the LBNs with samples in aqueous solution and freeze-dried LBNs containing sucrose for cryoprotection. Samples were stored under light exposure and at room temperature to examine a storage scenario that exposes CBD to an environment that promotes degradation. Fig. 2B shows the course of CBD loss in the samples over a time frame of six months. 97 ± 1% of CBD could be preserved in lyophilized archaeosomes after six months of storage, while only 24 ± 3% of CBD could be recovered in lyophilized SPC/Chol liposomes.

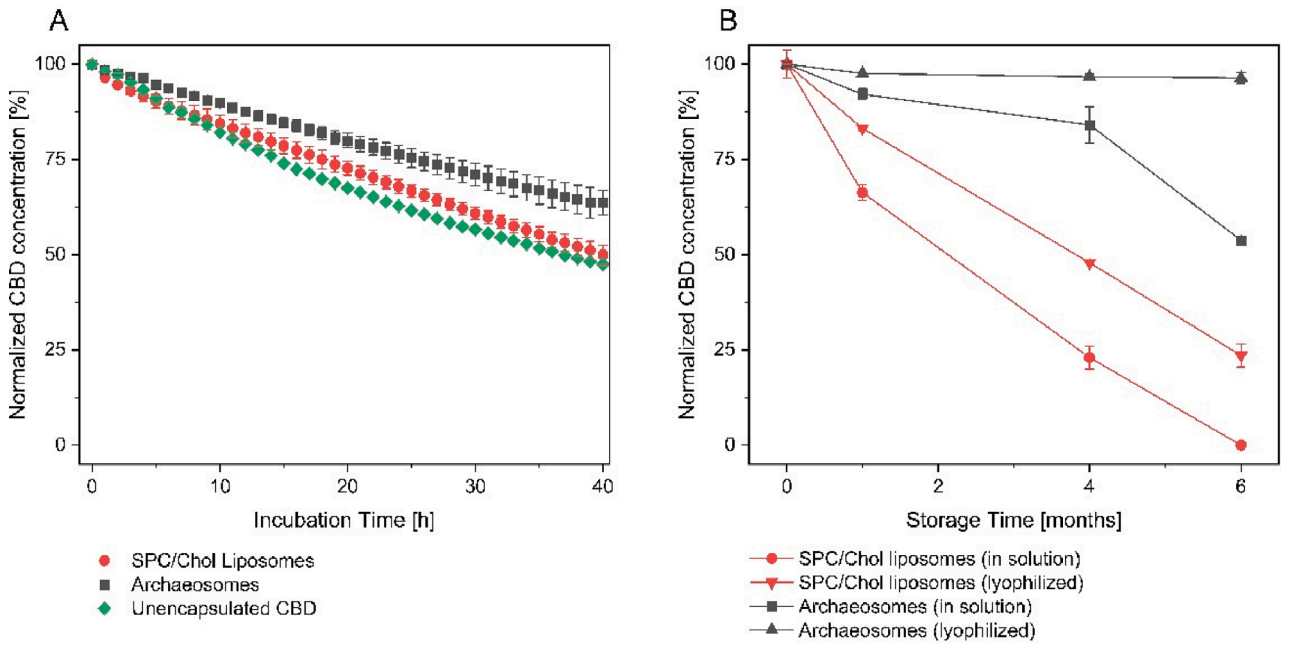

Fig. 2. Storage conditions tested in this study. (A) Accelerated oxidation study of soybean lecithin-based liposomes (SPC/Chol liposomes) archaeosomes, and unencapsulated cannabidiol (CBD); (B) Long-term storage over six months of lyophilized lipid-based nanocarriers (LBNs) containing sucrose as a cryoprotectant and LBNs in solution. CBD concentration over time was normalized to the initial concentration (t = 0) as the payload for SPC/Chol liposomes and archaeosomes differed. Normalized CBD concentration of SPC/Chol liposomes after six months was below the limit of quantification. All data represent the results of the HPLC measurement of three individual formulations for every sample.

Lyophilization of the LBNs provided stability to CBD compared to storage in solution (54 ± 1% of initial CBD content for archaeosomes in solution after six months, CBD concentration below limit of quantification for SPC/Chol liposomes). The size and PDI of the LBNs can be found in the Table S1 (Supplementary Material).

The advantages of archaeosomes regarding storage stability can be ascribed to structural and chemical differences. Monolayer-spanning tetraether lipids found in archaeosomes provide a high membrane rigidity, ensuring firmness and limited diffusion of CBD. Conventional lipid bilayers composed of soy lecithin-derived phospholipids lack this intrinsic rigidity (Takechi-Haraya et al., 2016). Consequently, cholesterol is added to unsaturated phosphatidylcholine-based formulations (Song et al., 2022). However, cholesterol is prone to oxidation under air exposure, restricting the long-term stability of LBNs. Moreover, SPC is rich in unsaturated linoleic acid (Weber, 1981). Hence, SPC-derived liposomes are highly susceptible to oxidation, restricting long-term storage. Drug leakage and fusion are potentially the main factors for the higher CBD degradation of SPC/Chol liposomes.

In contrast, saturated archaeal lipids are resistant to oxidation and hydrolysis due to ether bonds. Archaeosomes show enhanced physical and chemical stability, minimizing fusion and aggregation (Adamiak et al., 2021; Kaur et al., 2016). As these processes are kept to a minimum in lyophilized samples, freeze-drying of archaeosomes enables the storage of LBNs for six months with minor drug loss. Besides, the differences in Zeta potential, causing a higher repulsion of LBNs, may further contribute to a lower aggregation rate of archaeosomes in solution (Patil et al., 2007).

3.3. Stability of CBD liposomes and archaeosomes in a simulated digestion system

Essential for the applicability of an oral formulation is its stability in the GI tract, ultimately affecting the bioavailability of the cargo. CBD reportedly exhibits low stability in simulated gastric and physiological fluids (Merrick et al., 2016), suggesting the demand for an oral delivery system that reasonably protects the compound in the GI environment. In a simulated GI tract (Brodkorb et al., 2019), we compared the stability of SPC/Chol liposomes and archaeosomes, investigating their tolerance against simulated oral (SSF), gastric (SGF), and intestinal fluids (SIF) under physiological conditions. In all fluids, archaeosomes provide enhanced protection against CBD decay (Fig. 3). Degradation in oral

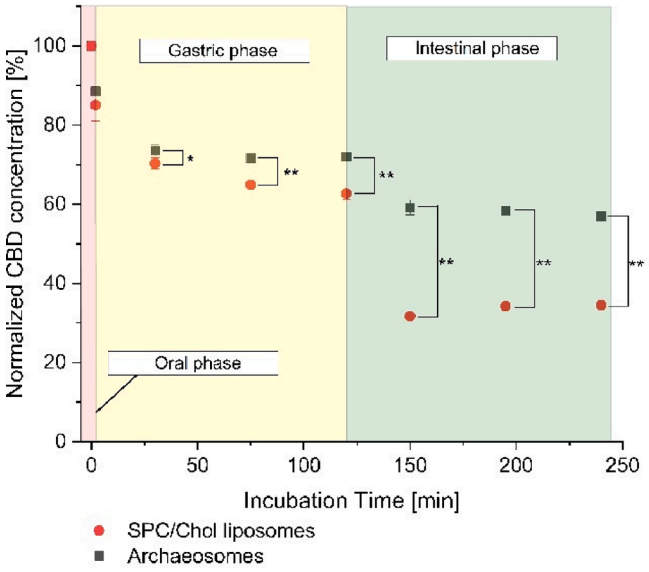

Fig. 3. Simulated GI tract of soybean lecithin-based liposomes (SPC/Chol liposomes) and archaeosomes. Three steps and simulated fluids are considered: oral (orange), gastric (yellow), and intestinal (green) phases. Lower decay of cannabidiol (CBD) shows the enzymatic and chemical stability of archaeosomes over SPC/Chol Liposomes. CBD concentration over time was normalized to the initial concentration (t = 0) as the payload for SPC/Chol liposomes and archaeosomes differed. All data represent the results of the HPLC measurement of three individual formulations for every sample. Statistical significance was calculated by unpaired Student's *t*-test (*P < 0.05; ** P < 0.01).

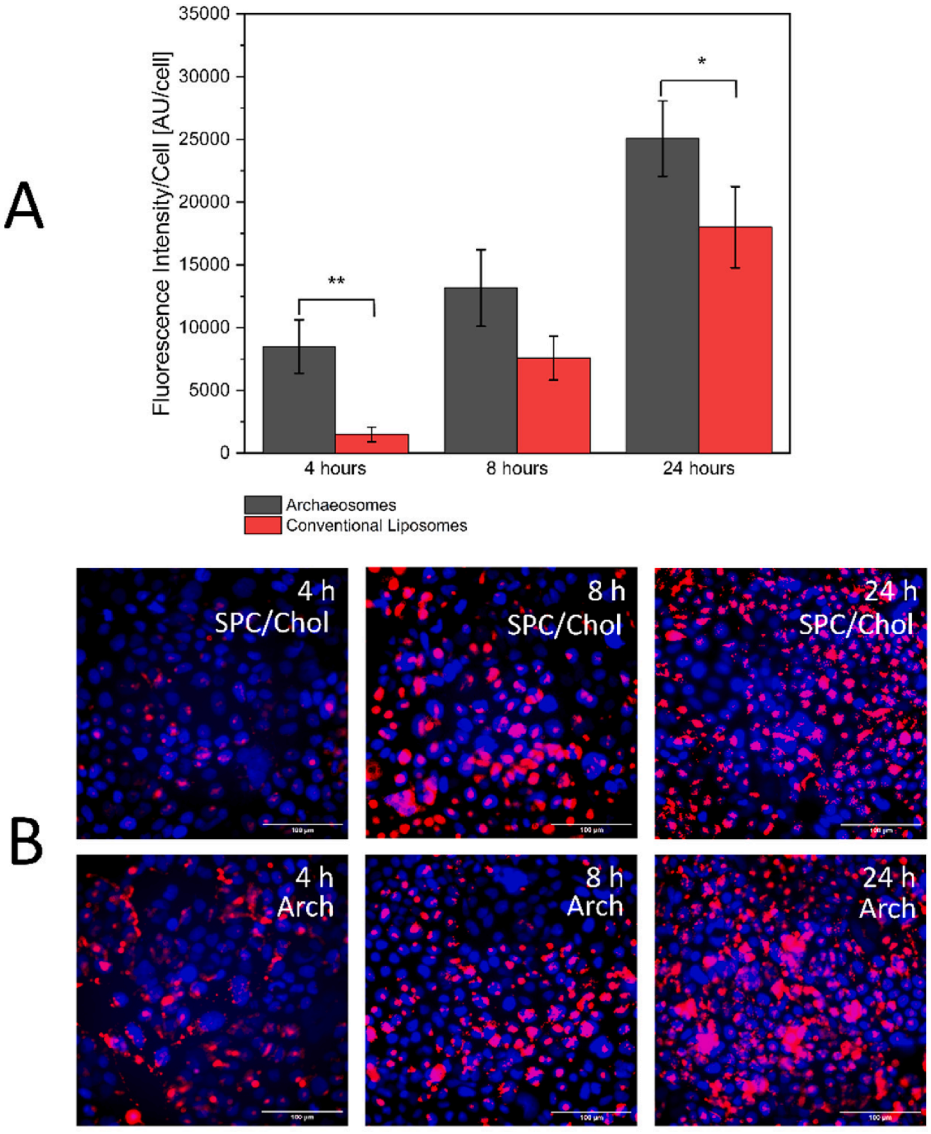

Fig. 4. *In vitro* particle uptake of soybean-based liposomes (SPC/Chol) and archaeosomes (Arch) after simulated digestion system. (A) Quantification of particle uptake in Caco-2 cells. The measurement of fluorescence intensity of rhodamine corresponds to the uptake of particles; the number of cells was assessed via Hoechst staining. (B) Kinetics of *in vitro* particle uptake of SPC/Chol liposomes (upper images) and archaeosomes (lower images). Microscopic images in 40x magnification of particle uptake after 4 h (left), 8 h (middle), and 24 h (right). Hoechst stain of cell nuclei is depicted in blue, and Rhodamine-labeled particles are displayed in red. The scale bar corresponds to 100 μm. Statistical significance was calculated by unpaired Student's *t*-test (* $P \leq 0.05$; ** $P \leq 0.01$).

fluids was similar for both LBNs, causing the loss of 15 ± 1% (SPC/Chol liposomes) and 11 ± 4% (archaeosomes) of CBD. Transfer of the samples to SGF again caused a similar decrease for both LBNs (~15%). The rapid decline can be explained by the acidic degradation of CBD encapsulated close to the surface of the LBNs. Lipolysis through gastric lipases and acidic hydrolysis of phosphatidylcholine probably cause the degradation of liposomes and explain the further CBD loss over the remaining 90 min in the gastric phase in SPC/Chol liposomes (68 ± 1% to 61 ± 1%). Resistance against esterases results in the stability of archaeosomes in the SGF environment without any further decay of CBD.

Interestingly, the transfer to SIF had the most significant effect on SPC/Chol liposomes. Bile salts disrupt lipid bilayers, while pancreatic enzymes further degrade liposomal structure (He et al., 2018). Archaeosomes were resistant to such conditions. While there is sufficient evidence in the literature to support that bile salts-lecithin mixed micelles are good solvents for lipophilic drugs (Müller et al., 2019; Dongowski et al., 2005), the stability of CBD in such systems was limited (Fig. 3). Archaeosomes, conversely, are believed to surpass the GI tract as intact colloidal structures (Morilla et al., 2011; Romero and Morilla, 2023). Hence, protection against harsh conditions in the GI tract is granted. At the end of the simulated GI tract, 57 ± 3% of CBD could be recovered in archaeosomal formulations, while only 34 ± 1% could be retrieved for SPC/Chol liposomal samples. Hence, archaeosomes grant higher protection against the milieu found in the observed fluids, while the loss of membrane integrity leads to extensive degradation in the case of SPC/Chol liposomes.

3.4. *In vitro uptake of CBD liposomes and archaeosomes in Caco-2 cells*

The intestinal epithelium is the primary physiological barrier that regulates the absorption of orally administered drugs (Zhang et al., 2014). Therapeutics can be transported via two pathways: 1.) transcellular transport via endocytosis/transcytosis in M cells or conventional enterocytes, and 2.) paracellular transport via tight junctions. In this study, we aimed to evaluate the degree of transcellular transport by assessing particle uptake of fluorescence-labeled LBNs via endocytosis.

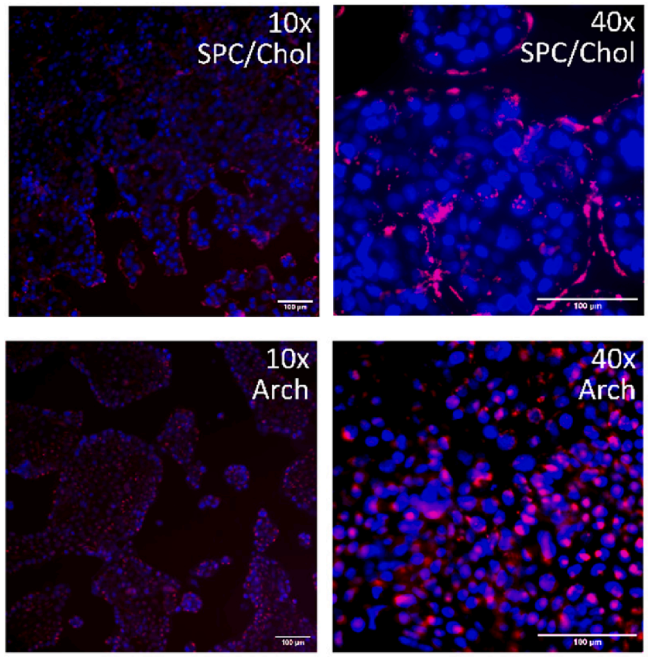

Fig. 5. Microscope images in 10x (left) and 40x (right) magnification of *in vitro* particle uptake of lyophilized soybean slecithin-based liposomes (SPC/Chol) (upper images) and archaeosomes (Arch) (lower images) after 8 h. In blue, stained nuclei are depicted; Rhodamine-labeled liposomes are visualized in red. Fluorescence signal of rhodamine in archaeosomal samples can be detected close to the cell nuclei, a significant proportion of rhodamine was observed on the outer surface for SPC/Chol liposomes.

Physiologically, liposomal phospholipids are digested to form lysoderivates and fatty acids in the GI tract. The degradation causes liposomes to lose their colloidal structure, and endocytosis occurs as mixed micelles. Lysoderivates activate chylomicrons, triggering exocytosis (Porter et al., 2007). In the case of archaeosomes, the transport mechanism is yet not understood, but a paracellular transportation has been considered as a potential uptake route (Romero and Morilla, 2023) besides a drug leakage involving adsorption of the LBNs to enterocytes (Parmentier et al., 2011).

The incorporation of 16:0 Liss Rhod PE did not affect the particle size of SPC/Chol liposomes (size = 79 ± 6; PDI = 0.108 ± 0.006) and archaeosomes (size = 87 ± 3 nm; PDI = 0.059 ± 0.015) and allowed the obtainment of a fluorescence signal inside the cells upon successful uptake. To evaluate the endocytosis of the LBNs quantitatively, we observed LBNs directly after preparation and after storage for six months. Fig. 4A shows the course of the fluorescence intensity normalized by the number of cells per image at the three sampling time points of LBNs after a completed simulated digestion system. After 4 h, a 6-fold enhanced signal was recognized, while we obtained a 1.7-fold respectively, 1.4-fold increased signal after 8 h and 24 h. Archaeosomes are endocytosed faster and to a greater extent. The differences between SPC/Chol liposomes and archaeosomes flatten throughout the study, which can be associated with a saturation effect caused by Caco-2 cells reaching a state close to confluency and high particle uptake in all cells (Fig. 4B).

To evaluate the particle uptake upon storage, we performed the assay of lyophilized LBNs and LBNs in solution after six months of storage. Fig. 5 shows images of lyophilized LBNs in 10x magnification. For SPC/Chol liposomes, we noticed a high degree of fluorescence signal on the outer layer of cells, suggesting non-successful endocytosis of LBNs. For archaeosomal samples, the fluorescence signal was located near the nuclei of Caco-2 cells, indicating the uptake of the particles by cells. Thus, no quantitative comparison, as done in Fig. 4, could be performed. The results underline the findings regarding stability discussed above, where archaeosomes were found to maintain their integrity over six months. Moreover, archaeosomes stored in an aqueous or lyophilized solution achieved successful endocytosis after storage at room temperature for six months.

Particle transport is a highly complex process involving multiple factors, including particle size and surface charge (Patil et al., 2007). While the particle size of the different LBNs in this study did not differ significantly, Zeta potential may be one factor that contributes to the higher uptake. Conventional liposomes have been described to follow caveolin-mediated endocytosis. In the case of archaeosomes, a detailed description of their interaction with enterocytes is missing, causing a hand full of speculations considering the mechanism behind cellular uptake. It is claimed that cellular transport occurs via one of the known endocytosis routes, namely caveolin, clathrin, or pinocytic pathways (Romero and Morilla, 2023). The *in vitro* uptake assay in this study suggests an accelerated and greater degree of endocytosis of archaeosomes. The success of lyophilized archaeosomes enables archaeosomal formulations to compete with current oral CBD oil formulations with the potential benefit of lowering the necessary dose due to stability reasons in the GI tract.

4. Conclusion

Besides two approved oil formulations, CBD's high potency and versatility promise its therapeutic use for various clinical conditions. However, oral administration of CBD, the most common route of drug delivery, comes with several hindrances. High clearance rates and low stability in the GI tract lead to a current bioavailability of only 6%. LBNs have shown that they can improve the bioavailability of lipophilic drugs due to higher dissolution, stability reasons, and uptake via the lymphatic system. Liposomal CBD is already found in commerce for food supplementation purposes.

We showed the enhanced chemical, physical and physiological stability of CBD-loaded archaeosomes compared to conventionally used phosphatidylcholine-based liposomes. Archaeosomes exposed significant advantages considering payload concentration, storage stability, and protection against cargo oxidation. Moreover, they showed high stability in a simulated GI tract and enabled an increased uptake by up to 6-fold of archaeosomes compared to SPC/Chol liposomes using Caco-2 as an enterocyte model cell line. Approved CBD oil products Epidiolex® (100 mg/mL CBD) and Sativex® (27 mg/mL Δ^9-THC; 25 mg/mL CBD) contain high concentrations of cannabinoids. Our results encourage that archaeosomal formulations could lower such high dosing due to a higher GI stability while granting a high particle uptake. Lyophilization of CBD archaeosomes ensures long-term storage and enables LBNs to compete with high-dose CBD products. The mechanism of archaeosome transportation is yet not understood, but the absence of hydrolysis products, as is the case for conventional liposomes, suggests relatively poor chylomicron-mediated exocytosis. This implies a lower dependency on food effects than commercial CBD oil products and conventional liposomes, further enhancing patient adherence.

CRediT authorship contribution statement

Viktor Sedlmayr: Conceptualization, Methodology, Investigation, Writing – original draft, Visualization. **Christina Horn:** Conceptualization, Methodology, Investigation. **David Johannes Wurm:** Writing – review & editing. **Oliver Spadiut:** Conceptualization, Funding acquisition, Project administration, Supervision, Writing – review & editing. **Julian Quehenberger:** Conceptualization, Supervision, Writing – review & editing.

Declaration of Competing Interest

The authors declare the following financial interests/personal relationships which may be considered as potential competing interests:

David J. Wurm reports writing assistance was provided by NovoArc GmbH. Viktor Sedlmayr, Christina Horn reports equipment, drugs, or supplies was provided by NovoArc GmbH. Viktor Sedlmayr, Christina Horn reports a relationship with NovoArc GmbH that includes: employment. David J. Wurm, Julian Quehenberger reports a relationship with NovoArc GmbH that includes: employment and equity or stocks. Oliver Spadiut reports a relationship with NovoArc GmbH that includes: consulting or advisory and equity or stocks. David J. Wurm, Oliver Spadiut, Julian Quehenberger has patent #EP3937901B1 licensed to NovoArc GmbH.

Data availability

Data will be made available on request.

Acknowledgments

The authors acknowledge the Austrian Science Fund (FWF) for funding via the project "CO2 fixation in extreme conditions" (Project Nr.: I 4508). The authors thank Silvia Schobesberger, Sarah Spitz, and Peter Ertl for their help establishing the *in vitro* uptake assay in Caco-2 cells. The authors thank Thomas Heuser from the Vienna BioCenter Core Facilities (VBCF) for cryo-TEM analysis. The graphical abstract was created with BioRender.com.

Appendix A. Supplementary data

Supplementary data to this article can be found online at https://doi.org/10.1016/j.ijpharm.2023.123434.

References

Abichabki, N., Zacharias, L.V., Moreira, N.C., Bellissimo-Rodrigues, F., Moreira, F.L., Benzi, J.R.L., Ogasawara, T.M.C., Ferreira, J.C., Ribeiro, C.M., Pavan, F.R., Pereira, L.R.L., Brancini, G.T.P., Braga, G.Ú.L., Zuardi, A.W., Hallak, J.E.C., Crippa, J.A.S., Lanchote, V.L., Cantón, R., Darini, A.L.C., Andrade, L.N., 2022. Potential cannabidiol (CBD) repurposing as antibacterial and promising therapy of CBD plus polymyxin B (PB) against PB-resistant gram-negative bacilli. Sci. Rep. 12, 6454. https://doi.org/10.1038/s41598-022-10393-8.

Adamiak, N., Krawczyk, K.T., Locht, C., Kowalewicz-Kulbat, M., 2021. Archaeosomes and Gas Vesicles as Tools for Vaccine Development. Front, Immunol, p. 12.

Ahn, H., Park, J.-H., 2016. Liposomal delivery systems for intestinal lymphatic drug transport. Biomater. Res. 20, 36. https://doi.org/10.1186/s40824-016-0083-1.

Alqahtani, M.S., Kazi, M., Alsenaidy, M.A., Ahmad, M.Z., 2021. Advances in oral drug delivery. Front. Pharmacol. 12, 618411 https://doi.org/10.3389/fphar.2021.618411.

Atalay, S., Jarocka-Karpowicz, I., Skrzydlewska, E., 2019. Antioxidative and anti-inflammatory properties of cannabidiol. Antioxidants 9, 21. https://doi.org/10.3390/antiox9010021.

Birnbaum, A.K., Karanam, A., Marino, S.E., Barkley, C.M., Remmel, R.P., Roslawski, M., Gramling-Aden, M., Leppik, I.E., 2019. Food effect on pharmacokinetics of cannabidiol oral capsules in adult patients with refractory epilepsy. Epilepsia 60, 1586–1592. https://doi.org/10.1111/epi.16093.

Blaskovich, M.A.T., Kavanagh, A.M., Elliott, A.G., Zhang, B., Ramu, S., Amado, M., Lowe, G.J., Hinton, A.O., Pham, D.M.T., Zuegg, J., Beare, N., Quach, D., Sharp, M.D., Pogliano, J., Rogers, A.P., Lyras, D., Tan, L., West, N.P., Crawford, D.W., Peterson, M.L., Callahan, M., Thurn, M., 2021. The antimicrobial potential of cannabidiol. Commun. Biol. 4, 7. https://doi.org/10.1038/s42003-020-01530-y.

Brodkorb, A., Egger, L., Alminger, M., Alvito, P., Assunção, R., Ballance, S., Bohn, T., Bourlieu-Lacanal, C., Boutrou, R., Carrière, F., Clemente, A., Corredig, M., Dupont, D., Dufour, C., Edwards, C., Golding, M., Karakaya, S., Kirkhus, B., Feunteun, S.L., Lesmes, U., Macierzanka, A., Mackie, A.R., Martins, C., Marze, S., McClements, D.J., Ménard, O., Minekus, M., Portmann, R., Santos, C.N., Souchon, I., Singh, R.P., Vegarud, G.E., Wickham, M.S.J., Weitschies, W., Recio, I., 2019. INFOGEST static in vitro simulation of gastrointestinal food digestion. Nat. Protoc. 14, 991–1014. https://doi.org/10.1038/s41596-018-0119-1.

Chong, P.-L.-G., Chang, A., Yu, A., Mammedova, A., 2022. Vesicular and planar membranes of archaea lipids: unusual physical properties and biomedical applications. Int. J. Mol. Sci. 23, 7616. https://doi.org/10.3390/ijms23147616.

Citti, C., Russo, F., Linciano, P., Strallhofer, S.S., Tolomeo, F., Forni, F., Vandelli, M.A., Gigli, G., Cannazza, G., 2021. Origin of Δ^{9}-Tetrahydrocannabinol Impurity in Synthetic Cannabidiol. Cannabis Cannabinoid Res. 6, 28–39. https://doi.org/10.1089/can.2020.0021.

Cristino, L., Bisogno, T., Di Marzo, V., 2020. Cannabinoids and the expanded endocannabinoid system in neurological disorders. Nat. Rev. Neurol. 16, 9–29. https://doi.org/10.1038/s41582-019-0284-z.

Crommelin, D.J.A., Van Hoogevest, P., Storm, G., 2020. The role of liposomes in clinical nanomedicine development. What now? Now what? J. Control. Release 318, 256–263. https://doi.org/10.1016/j.jconrel.2019.12.023.

Dongowski, G., Fritzsch, B., Giessler, J., Härtl, A., Kuhlmann, O., Neubert, R.H.H., 2005. The influence of bile salts and mixed micelles on the pharmacokinetics of quinine in rabbits. Eur. J. Pharm. Biopharm. 60, 147–151. https://doi.org/10.1016/j.ejpb.2005.01.003.

Franco, V., Gershkovich, P., Perucca, E., Bialer, M., 2020. The interplay between liver first-pass effect and lymphatic absorption of cannabidiol and its implications for cannabidiol oral formulations. Clin. Pharmacokinet. 59, 1493–1500. https://doi.org/10.1007/s40262-020-00931-w.

Fricker, G., Kromp, T., Wendel, A., Blume, A., Zirkel, J., Rebmann, H., Setzer, C., Quinkert, R.-O., Martin, F., Müller-Goymann, C., 2010. Phospholipids and lipid-based formulations in oral drug delivery. Pharm. Res. 27, 1469–1486. https://doi.org/10.1007/s11095-010-0130-x.

Golombek, P., Müller, M., Barthlott, I., Sproll, C., Lachenmeier, D.W., 2020. Conversion of cannabidiol (CBD) into psychotropic cannabinoids including tetrahydrocannabinol (THC): a controversy in the scientific literature. Toxics 8, 41. https://doi.org/10.3390/toxics8020041.

He, H., Lu, Y., Qi, J., Zhu, Q., Chen, Z., Wu, W., 2018. Adapting liposomes for oral drug delivery. Acta Pharm. Sin. B. https://doi.org/10.1016/j.apsb.2018.06.005.

Hemetsberger, A., Preis, E., Engelhardt, K., Gutberlet, B., Runkel, F., Bakowsky, U., 2022. Highly stable liposomes based on tetraether lipids as a promising and versatile drug delivery system. Materials 15, 6995. https://doi.org/10.3390/ma15196995.

Hinz, B., Ramer, R., 2019. Anti-tumour actions of cannabinoids: Anti-tumour actions of cannabinoids. Br. J. Pharmacol. 176, 1384–1394. https://doi.org/10.1111/bph.14426.

Itin, C., Domb, A.J., Hoffman, A., 2019. A meta-opinion: cannabinoids delivered to oral mucosa by a spray for systemic absorption are rather ingested into gastro-intestinal tract: the influences of fed / fasting states. Expert Opin. Drug Deliv. 16, 1031–1035. https://doi.org/10.1080/17425247.2019.1653852.

Jia, Y., Agbayani, G., Chandan, V., Iqbal, U., Dudani, R., Qian, H., Jakubek, Z., Chan, K., Harrison, B., Deschatelets, L., Akache, B., McCluskie, M.J., 2022. Evaluation of adjuvant activity and bio-distribution of archaeosomes prepared using microfluidic technology. Pharmaceutics 14, 2291. https://doi.org/10.3390/pharmaceutics14112291.

Kaur, G., Garg, T., Rath, G., Goyal, A.K., 2016. Archaeosomes: an excellent carrier for drug and cell delivery. Drug Deliv. 23, 2497–2512. https://doi.org/10.3109/10717544.2015.1019653.

Khadke, S., Roces, C.B., Donaghey, R., Giacobbo, V., Su, Y., Perrie, Y., 2020. Scalable solvent-free production of liposomes. J. Pharm. Pharmacol. 72, 1328–1340. https://doi.org/10.1111/jphp.13329.

Khodadadi, H., Salles, É.L., Jarrahi, A., Chibane, F., Costigliola, V., Yu, J.C., Vaibhav, K., Hess, D.C., Dhandapani, K.M., Baban, B., 2020. Cannabidiol modulates cytokine storm in acute respiratory distress syndrome induced by simulated viral infection using synthetic RNA. Cannabis Cannabinoid Res. 5, 197–201. https://doi.org/10.1089/can.2020.0043.

Kok, L.Y., Bannigan, P., Sanaee, F., Evans, J.C., Dunne, M., Regenold, M., Ahmed, L., Dubins, D., Allen, C., 2022. Development and pharmacokinetic evaluation of a self-nanoemulsifying drug delivery system for the oral delivery of cannabidiol. Eur. J. Pharm. Sci. 168, 106058 https://doi.org/10.1016/j.ejps.2021.106058.

Li, Z., Chen, J., Sun, W., Xu, Y., 2010. Investigation of archaeosomes as carriers for oral delivery of peptides. Biochem. Biophys. Res. Commun. 394, 412–417. https://doi.org/10.1016/j.bbrc.2010.03.041.

Lin, L., Wong, H., 2017. Predicting oral drug absorption: mini review on physiologically-based pharmacokinetic models. Pharmaceutics 9, 41. https://doi.org/10.3390/pharmaceutics9040041.

Mastronarde, D.N., 2005. Automated electron microscope tomography using robust prediction of specimen movements. J. Struct. Biol. 152, 36–51. https://doi.org/10.1016/j.jsb.2005.07.007.

Mechoulam, R., Hanuš, L., 2002. Cannabidiol: an overview of some chemical and pharmacological aspects. Part I: chemical aspects. Chem. Phys. Lipids 121, 35–43. https://doi.org/10.1016/S0009-3084(02)00144-5.

Merrick, J., Lane, B., Sebree, T., Yaksh, T., O'Neill, C., Banks, S.L., 2016. Identification of psychoactive degradants of cannabidiol in simulated gastric and physiological fluid. Cannabis Cannabinoid Res. 1, 102–112. https://doi.org/10.1089/can.2015.0004.

Millar, S.A., Maguire, R.F., Yates, A.S., O'Sullivan, S.E., 2020. Towards Better Delivery of Cannabidiol (CBD). Pharmaceuticals 13, 219. https://doi.org/10.3390/ph13090219.

Morilla, M.J., Mengual Gomez, D., Cabral, P., Cabrera, M., Balter, H., Victoria Defain Tesoriero, M., Higa, L., Roncaglia, D., L Romero, E., 2011. M Cells Prefer Archaeosomes: An In Vitro/In Vivo Snapshot Upon Oral Gavage in Rats [WWW Document]. https://doi.org/info:doi/10.2174/156720111795256138.

Müller, S., Gruhle, K., Meister, A., Hause, G., Drescher, S., 2019. Bolalipid-doped liposomes: can bolalipids increase the integrity of liposomes exposed to gastrointestinal fluids? Pharmaceutics 11, 646. https://doi.org/10.3390/pharmaceutics11120646.

Nakhaei, P., Margiana, R., Bokov, D.O., Abdelbasset, W.K., Jadidi Kouhbanani, M.A., Varma, R.S., Marofi, F., Jarahian, M., Beheshtkhoo, N., 2021. Liposomes: structure, biomedical applications, and stability parameters with emphasis on cholesterol. Front. Bioeng. Biotechnol. 9, 705886 https://doi.org/10.3389/fbioe.2021.705886.

Pacifici, R., Marchei, E., Salvatore, F., Guandalini, L., Busardò, F.P., Pichini, S., 2017. Evaluation of cannabinoids concentration and stability in standardized preparations of cannabis tea and cannabis oil by ultra-high performance liquid chromatography tandem mass spectrometry. Clin. Chem. Lab. Med. CCLM 55. https://doi.org/10.1515/cclm-2016-1060.

Parmentier, J., Thewes, B., Gropp, F., Fricker, G., 2011. Oral peptide delivery by tetraether lipid liposomes. Int. J. Pharm. 415, 150–157. https://doi.org/10.1016/j.ijpharm.2011.05.066.

Parmentier, J., Hofhaus, G., Thomas, S., Cuesta, L.C., Gropp, F., Schröder, R., Hartmann, K., Fricker, G., 2014. Improved oral bioavailability of human growth hormone by a combination of liposomes containing bio-enhancers and tetraether lipids and omeprazole. J. Pharm. Sci. 103, 3985–3993. https://doi.org/10.1002/jps.24215.

Patil, S., Sandberg, A., Heckert, E., Self, W., Seal, S., 2007. Protein adsorption and cellular uptake of cerium oxide nanoparticles as a function of zeta potential. Biomaterials 28, 4600–4607. https://doi.org/10.1016/j.biomaterials.2007.07.029.

Perucca, E., Bialer, M., 2020. Critical aspects affecting cannabidiol oral bioavailability and metabolic elimination, and related clinical implications. CNS Drugs 34, 795–800. https://doi.org/10.1007/s40263-020-00741-5.

Porter, C.J.H., Trevaskis, N.L., Charman, W.N., 2007. Lipids and lipid-based formulations: optimizing the oral delivery of lipophilic drugs. Nat. Rev. Drug Discov. 6, 231–248. https://doi.org/10.1038/nrd2197.

Quehenberger, J., Pittenauer, E., Allmaier, G., Spadiut, O., 2020. The influence of the specific growth rate on the lipid composition of *Sulfolobus acidocaldarius*. Extremophiles. https://doi.org/10.1007/s00792-020-01165-1.

Rastädter, K., Wurm, D.J., Spadiut, O., Quehenberger, J., 2020. The cell membrane of *Sulfolobus* spp.—homeoviscous adaption and biotechnological applications. Int. J. Mol. Sci. 21, 3935. https://doi.org/10.3390/ijms21113935.

Romero, E.L., Morilla, M.J., 2023. Ether lipids from archaeas in nano-drug delivery and vaccination. Int. J. Pharm. 634, 122632 https://doi.org/10.1016/j.ijpharm.2023.122632.

Schilrreff, P., Simioni, Y.R., Jerez, H.E., Caimi, A.T., de Farias, M.A., Villares Portugal, R., Romero, E.L., Morilla, M.J., 2019. Superoxide dismutase in nanoarchaeosomes for targeted delivery to inflammatory macrophages. Colloids Surf. B Biointerfaces 179, 479–487. https://doi.org/10.1016/j.colsurfb.2019.03.061.

Schneider, C.A., Rasband, W.S., Eliceiri, K.W., 2012. NIH Image to ImageJ: 25 years of image analysis. Nat. Methods 9, 671–675. https://doi.org/10.1038/nmeth.2089.

Shen, S., Wu, Y., Liu, Y., Wu, D., 2017. High drug-loading nanomedicines: progress, current status, and prospects. Int. J. Nanomed. 12, 4085–4109. https://doi.org/10.2147/IJN.S132780.

Silvestro, S., Mammana, S., Cavalli, E., Bramanti, P., Mazzon, E., 2019. Use of cannabidiol in the treatment of epilepsy: efficacy and security in clinical trials. Molecules 24, 1459. https://doi.org/10.3390/molecules24081459.

Singh, A., Neupane, Y.R., Shafi, S., Mangla, B., Kohli, K., 2020. PEGylated liposomes as an emerging therapeutic platform for oral nanomedicine in cancer therapy: in vitro and in vivo assessment. J. Mol. Liq. 303, 112649 https://doi.org/10.1016/j.molliq.2020.112649.

Song, F., Chen, J., Zheng, A., Tian, S., 2022. Effect of sterols on liposomes: Membrane characteristics and physicochemical changes during storage. LWT 164, 113558. https://doi.org/10.1016/j.lwt.2022.113558.

Takechi-Haraya, Y., Sakai-Kato, K., Abe, Y., Kawanishi, T., Okuda, H., Goda, Y., 2016. Atomic force microscopic analysis of the effect of lipid composition on liposome membrane rigidity. Langmuir 32, 6074–6082. https://doi.org/10.1021/acs.langmuir.6b00741.

Thomas, A., Baillie, G.L., Phillips, A.M., Razdan, R.K., Ross, R.A., Pertwee, R.G., 2007. Cannabidiol displays unexpectedly high potency as an antagonist of CB_1 and CB_2 receptor agonists *in vitro*: Cannabinoid antagonism by cannabidiol. Br. J. Pharmacol. 150, 613–623. https://doi.org/10.1038/sj.bjp.0707133.

Tiboni, M., Tiboni, M., Pierro, A., Del Papa, M., Sparaventi, S., Cespi, M., Casettari, L., 2021. Microfluidics for nanomedicines manufacturing: An affordable and low-cost 3D printing approach. Int. J. Pharm. 599, 120464 https://doi.org/10.1016/j.ijpharm.2021.120464.

Uhl, P., Helm, F., Hofhaus, G., Brings, S., Kaufman, C., Leotta, K., Urban, S., Haberkorn, U., Mier, W., Fricker, G., 2016. A liposomal formulation for the oral application of the investigational hepatitis B drug Myrcludex B. Eur. J. Pharm. Biopharm. 103, 159–166. https://doi.org/10.1016/j.ejpb.2016.03.031.

Weber, E.J., 1981. Compositions of commercial corn and soybean lecithins. J. Am. Oil Chem. Soc. 58, 898–901. https://doi.org/10.1007/BF02659654.

Zhang, J., Zhu, X., Jin, Y., Shan, W., Huang, Y., 2014. Mechanism study of cellular uptake and tight junction opening mediated by goblet cell-specific trimethyl chitosan nanoparticles. Mol. Pharm. 11, 1520–1532. https://doi.org/10.1021/mp400685v.